

This is a repository copy of *Extracellular vesicle microRNA cargo is correlated with HPV status in oropharyngeal carcinoma*.

White Rose Research Online URL for this paper: http://eprints.whiterose.ac.uk/140646/

Version: Accepted Version

Article:

Peacock, B., Rigby, A., Bradford, J. orcid.org/0000-0002-7771-914X et al. (4 more authors) (2018) Extracellular vesicle microRNA cargo is correlated with HPV status in oropharyngeal carcinoma. Journal of Oral Pathology and Medicine, 47 (10). pp. 954-963. ISSN 0904-2512

https://doi.org/10.1111/jop.12781

This is the peer reviewed version of the following article: Peacock B, Rigby A, Bradford J, et al. Extracellular vesicle microRNA cargo is correlated with HPV status in oropharyngeal carcinoma. J Oral Pathol Med. 2018;47:954–963, which has been published in final form at https://doi.org/10.1111/jop.12781. This article may be used for non-commercial purposes in accordance with Wiley Terms and Conditions for Use of Self-Archived Versions.

Reuse

Items deposited in White Rose Research Online are protected by copyright, with all rights reserved unless indicated otherwise. They may be downloaded and/or printed for private study, or other acts as permitted by national copyright laws. The publisher or other rights holders may allow further reproduction and re-use of the full text version. This is indicated by the licence information on the White Rose Research Online record for the item.

Takedown

If you consider content in White Rose Research Online to be in breach of UK law, please notify us by emailing eprints@whiterose.ac.uk including the URL of the record and the reason for the withdrawal request.



DR STUART HUNT (Orcid ID: 0000-0001-5572-1030)

Article type : Original Article

Extracellular vesicle microRNA cargo is correlated with HPV-status in oropharyngeal carcinoma

Running title: EV miRNA cargo in OPSCC

Ben Peacock¹, Alice Rigby¹, James Bradford^{2,4}, Ryan Pink³, Keith Hunter¹, Daniel Lambert^{1,4} and Stuart Hunt¹

¹The School of Clinical Dentistry, The University of Sheffield, UK; ²Department of Oncology and Metabolism, Medical School, The University of Sheffield, UK; ³Department of Biological and Medical Sciences, Oxford Brookes University, UK; ⁴Sheffield Institute for Nucleic Acids, University of Sheffield, UK

Corresponding author: Dr Stuart Hunt, Unit of Oral and Maxillofacial Medicine, Surgery and Pathology, The School of Clinical Dentistry, The University of Sheffield, 19 Claremont Crescent, Sheffield, South Yorkshire, S10 2TA, UK.

Email: s.hunt@sheffield.ac.uk

This article has been accepted for publication and undergone full peer review but has not been through the copyediting, typesetting, pagination and proofreading process, which may lead to differences between this version and the Version of Record. Please cite this article as doi: 10.1111/jop.12781 This article is protected by copyright. All rights reserved. Keywords: Extracellular vesicles, microRNA, oropharyngeal carcinoma, human papillomavirus, head and neck cancer

Abstract

Background: The incidence of human papilloma virus positive (HPV⁺) oropharyngeal squamous cell carcinoma (OPSCC) has increased rapidly in recent decades. These tumours have a favourable outcome compared to HPV-negative (HPV⁻) OPSCC. However, HPV⁺ tumours are more likely to metastasise to distant sites, suggesting a difference in how these tumour subtypes interact with the metastatic niche. Extracellular vesicles (EVs) have emerged as important players in cell-to-cell communication and are a potential source of biomarkers for cancer diagnosis. This study aims to characterise the microRNA cargo of small EVs released by HPV⁺ and HPV⁻ OPSCC cell lines.

Methods: EVs produced by HPV⁺ (SCC2 and SCC90) and HPV⁻ (SCC72 an SCC89) OPSCC cells were characterised by tunable resistive pulse sensing (TRPS) and western blotting. RNA was extracted from EVs and analysed by small RNA sequencing. A bioinformatics approach was used to identify EV miRNA signatures associated with HPV status.

Results: HPV- OPSCC cells produced more EVs than HPV+ OPSCC cells. EVs were positive for the common EV markers CD63, CD9 and TSG101. Unbiased hierarchical clustering analysis of EV miRNA cargo revealed that samples clustered based on HPV status. 14 miRNA were enriched in HPV+ cell-derived EVs, whereas, 19 miRNA were enriched in EVs derived from HPV- cell lines.

Conclusions: Here we identify EV miRNA signatures indicative of the HPV status of the parent cell. This may provide a platform from which to validate salivary or blood-based biomarkers with utility for early detection and stratifying risk in OPSCC patients.

The incidence of human papillomavirus-positive (HPV+) oropharyngeal squamous cell carcinoma (OPSCC) has risen dramatically in recent decades. This is in contrast to HPV-negative (HPV-) OPSCC, which continues to decline.^{1,2} It has been predicted that by 2020 the annual incidence of HPV+ OPSCC will overtake the number of cervical cancers and will represent the majority of head and neck cancers by 2030.¹ HPV+ OPSCC have been shown to have a more favourable outcome due to an increased sensitivity to radiotherapy and lower risk of recurrence at the primary site when compared to HPV- OPSCC.³ However, some patients with HPV+ OPSCC have poor outcomes due to formation of distant metastases, which typically manifest later than in HPV- patients, can occur at unusual sites and may display a disseminating or explosive phenotype.⁴

Extracellular vesicles (EVs) are nanoscale, membrane enclosed vesicles released by cells to facilitate cell-to-cell communication.⁵ EVs contain molecular cargo such as nucleic acids and protein.⁶ They are present in all biological fluids⁷, have attracted much attention as a source of biomarkers for disease diagnosis and also as novel therapeutic targets, as their contents appear to be altered in disease.⁸

There is evidence that HPV alters the expression of host cell microRNAs⁹⁻¹¹ and the cargo of EVs released by cervical cancer cells.^{12,13} However, despite the common viral aetiology there are no similar studies in OPSCC. To address this gap in the literature, we characterised the small EVs released by HPV⁺ and HPV⁻ OPSCC cell lines and performed small RNA sequencing on EV cargo to elucidate the miRNA signature associated with these different tumours.

Cell culture – During this study four oropharyngeal carcinoma cell lines were used, which were received under Material Transfer Agreement from Prof. S. Gollin, University of Pittsburgh School of Public Health, Pittsburgh, PA: SCC2 (hypopharynx), SCC90 (base of tongue), SCC72 (tonsil) and SCC89 (tonsil). Two were HPV16 positive (SCC2 and SCC90) and two were HPV negative (SCC72 and SCC90). HPV status was confirmed by cytology testing carried out by the Directorate of Laboratory Medicine at The Royal Hallamshire Hospital, Sheffield Teaching Hospitals NHS Foundation Trust, Sheffield. Cell lines were routinely cultured in Dulbecco's Modified Eagle's Medium (DMEM) supplemented with 10% (v/v) FBS and 2 mM L-glutamine (all from Sigma-Aldrich, Dorset, UK). Cells were maintained at 37°C, 5% CO₂ in a humidified environment.

Conditioned medium and EV isolation - Cells were seeded in complete growth medium and allowed to adhere overnight. Monolayers were washed with PBS and the medium exchanged for DMEM supplemented with 5% (v/v) EV-depleted FBS (centrifuged at 100,000 x *g* for 18 hours and filtered through a 0.2 μ m syringe filter) and incubated for 24-72 h. Conditioned medium was centrifuged at 300 x *g* for 10 min, 2000 x *g* for 10 min, 10,000 x *g* for 30 min. The supernatant was concentrated to 0.5 ml using a Vivaspin-20 (100 MWCO) device (GE Healthcare, Buckinghamshire, UK). EVs were separated from soluble factors by size exclusion chromatography using Sepharose CL-2B (GE Healthcare, Uppsala, Sweden) stacked in disposable Econo-Pac columns (Biorad, Watford, UK) and eluted in PBS. Where required, EVs were pelleted by ultracentrifugation at 100,000 x *g* for 1 h.

Tunable resistive pulse sensing (TRPS) - EVs were analysed by TRPS using a qNano instrument (iZON, Oxford, UK). An NP100 nanopore was selected to measure small EVs. Typical settings were 45 mm stretch, 0.5 V, 10 mbar pressure, but small alterations were made as required to maintain a current of ~125 nA.

Western blotting - Cell and EV pellets were resuspended in RIPA buffer supplemented with protease inhibitor cocktail. Protein concentration was calculated by BCA assay (Thermo Fisher,Waltham, USA) and 20 µg of protein per sample was separated by SDS-PAGE on 10% polyacrylamide gels. Proteins were transferred to nitrocellulose membrane using the BioRad Turbo Blot system. Membranes were blocked for 1 h at room temperature in 5% (w/v) skimmed milk powder in TBST. Primary antibodies were added at the following dilutions at 4°C for 18 h: CD9 (EPR2949) 1:2000, CD63 (EPR5702) 1:500, TSG101 (51/TSG101) 1:1000, GM130 (EP892Y) 1:2000. Antibodies against CD9, CD63 and GM130 were purchased from Abcam (Cambridge, UK). The TSG101 antibody was purchased from BD Bioscience (New Jersey, USA). Membranes were washed three times with TBST for 10 min, followed by incubation with HRPconjugated secondary antibodies (Cell Signaling Technology, Massachusetts, USA) for 1 h at room temperature. Membranes were washed three times with TBST for 10 min, followed by incubation with ECL Pierce substrate (Thermo Fisher,Waltham, USA) and exposure to X-ray film (Thermo Fisher,Waltham, USA). Films were developed and fixed using a Compact X4 automatic processor (Xograph Imaging Systems, Stonehouse, UK).

Small RNA sequencing - EV pellets were resuspended in lysis buffer from the miRCURY RNA isolation kit (Exiqon, Vedbaek, Denmark) and the protocol was followed according to manufacturer's instructions, including the optional on-column DNase treatment. Small RNA sequencing was performed at the Clinical Research Facility, University of Edinburgh: RNA quality and integrity was determined by Agilent 2100 Bioanalyzer Instrument with the RNA 6000 Pico Kit. RNA concentration was quantified using the Qubit 2.0 fluorometer and the Qubit RNA HS Assay Kit. Library preparation was performed using the Ion Total RNA-Seq Kit v2. RNA was hybridised and ligated before being reverse transcribed to cDNA and purified using magnetic beads. cDNA was amplified with Ion Torrent adapters and barcodes for 18 cycles of PCR before being purified. Library yields were quantified using the Qubit 2.0 fluorometer and the dsDNA HS Kit. Libraries were combined in equimolar amounts for template preparation before sequencing on the Ion Proton Instrument on a P1 v3 chip. Output files were converted to BAM files by an automated workflow using the Torrent Suite software v5.0.4. In addition, the smallRNA_analysis plug-in v5.0.3.0 was used to analyse microRNA reads. Unmapped reads were aligned to the whole genome to rescue miRBase unaligned reads.

Quantitative real-time PCR - Cellular and EV RNA was reverse transcribed using the small RNA reverse transcription kit with the appropriate RT primer (Applied biosystems, California, USA). QPCR reactions consisted of Taqman mastermix, the appropriate primer/probe sets (Applied biosystems, California, USA) and cDNA from specific miRNA RT. QPCR was performed using a Rotor Gene Q thermal cycler (Qiagen, Hilden, Germany). Data was normalised to hsa-let-7a-5p (a miRNA expressed at constant levels according to our data) and expressed relative to the sample with lowest abundance/expression using the $\Delta\Delta$ Ct method.

Processing of small RNA sequencing data – Raw sequence reads were aligned to miRBase using the smallRNA_analysis plug-in v5.0.3.0 within Torrent Suite software v5.0.4. Any unmapped reads were further aligned to the whole genome to rescue miRBase unaligned reads. Raw counts across each miRNA were then input to a differential expression (DE) analysis workflow through the web app developed by the bioinformatics core, Center for Research Informatics (CRI), University of Chicago (https://gallery.shinyapps.io/DEApp/). Briefly, the four cell lines were grouped by HPV status and the raw counts normalized. An exclusion criteria of <50 reads

per Million (RPM) in at least 2 columns/cell lines reduced the number of miRNAs analysed from 575 to 233. DE analysis and pathway enrichments was then performed on raw count data from the two groups using DESeq2¹⁴ with a cutoff for log2 Fold Change (log2 FC) of at least 1.5 and a P value <0.05.

Pathway analysis - Experimentally validated miRNA targets were determined using miRTarBase v.8¹⁵ for HPV⁻/⁺ EV enriched sets. Transcripts targeted by multiple miRNA were analysed for pathway enrichment using DAVID^{16,17} to identify head and neck cancer-associated pathways. Stringency criteria were applied using Benjamini-Hochberg correction <0.05.

Results

HPV negative OPSCC cell lines produce more EVs

Prior to purification of OPSCC-derived EVs, we sought to characterise the size profile of small EVs present in conditioned medium. TRPS using a qNano instrument revealed numerous small particles, most likely EVs, between 50 to 150 nm in diameter (Fig 1). Conditioned medium derived from one of the HPV⁻ cell lines, SCC89, contained EVs with a larger modal diameter (Fig 1A) and a more normal size distribution. Conditioned medium from the other cells examined, both HPV⁺ and HPV⁻, contained EVs with a skewed normal distribution (Fig 1C). Normalisation of EV concentration in conditioned medium to the number of producing cells revealed that HPV⁻ cells produced up to two fold more than HPV⁺ cells (*P* value <0.05) (Fig 1B).

Isolation of small EVs from conditioned medium

Small EVs were isolated from the conditioned medium of OPSCC cell lines by a combined differential centrifugation and size exclusion chromatography (SEC) approach. EV-rich fractions were combined and EVs were pelleted by ultracentrifugation (100,000 x *g* for 1 h). Pelleted EVs were resuspended in 50 µl PBS or protein lysis buffer for subsequent TRPS or western blot analysis, respectively. TRPS confirmed the isolation of small EVs with similar modal diameters to the particles detected in conditioned medium (compare Fig 1A with Fig 2A). Analysis of the EV size profiles showed that all samples contained particles between 50 to 150 nm in diameter with a skewed normal distribution (Fig 2C). Interestingly, the size profile of purified SCC89 EVs was similar to the other samples, suggesting that a proportion of the EVs larger than 80 nm (present in conditioned medium samples) were eliminated during the purification procedure (Fig 2C). Western blot analysis revealed that EV lysates were positive for the EV markers CD63, CD9 or TSG101. Whereas, the Golgi marker GM130 was only detected in cell lysates (Fig 2B).

EVs isolated from OPSCC cell lines contain a variety of small RNA molecules

RNA was extracted from EV pellets and subjected to Bioanalyzer analysis, which showed that samples were enriched with small RNA species <200 nt in length (Fig 3A-D). Small RNA sequencing produced 8-13 million reads per sample, with 89-94% mapped to mirBase and the human genome. Of these mapped reads, 2-15% aligned to miRNA sequences. Other RNA species that were identified included mRNA, rRNA, tRNA, snoRNA, snRNA and lincRNA (Fig 3E). Raw counts were converted to reads per million (RPM). For each sample 343-443 unique miRNA were identified. 63-82 miRNA had high abundance (>1000 RPM), 73-92 miRNA had intermediate abundance (100-1000 RPM) and 117-133 miRNA had low abundance (10-100 RPM) (Fig 3F).

EV miRNA profile correlates with HPV status

MiRNA data was converted to log2 RPM and unbiased hierarchical clustering analysis revealed that the global EV miRNA signature correlated with HPV status, with SCC2 and SCC90 (HPV⁺) and SCC72 and SCC89 (HPV⁻) clustering together (Fig 3G). In order to identify specific miRNA associated with HPV status, fold difference was calculated between HPV⁺ and HPV⁻ groups using DEseq2, with a cutoff of 1.5 log2 fold change and *P* value of <0.05. 14 miRNA were identified that were enriched in EVs from HPV⁺ cells and 19 miRNA were identified that were enriched in EVs from HPV⁻ cells (Table 1). In addition, 9 miRNA were very abundant in all EV samples (>5000 RPM), independent of HPV status (Table 1). We next sought to validate small RNA sequencing data by quantitative real-time PCR (QPCR). miR-29b-3p and miR-20b-5p were chosen as miRNA that were enriched in EVs derived from HPV⁻ or HPV⁺ cells, respectively. The pattern of enrichment seen in small RNA sequencing data (Fig 4A,D) was also observed by QPCR analysis (Fig 4B,E). We also examined the cellular expression level of each miRNA, which showed that the EV abundance showed a similar trend to that of cellular expression (Fig 4C,F).

Pathway analysis

Due to certain miRNA being enriched in either EVs derived from HPV⁺ or HPV⁻ cells, we used a bioinformatics approach to determine which cell signalling pathways in the tumour microenvironment might be affected by cellular uptake of EVs released by cancer cells in OPSCC. In addition, we wanted to know if the analysis could elucidate which pathways were being dysregulated in cancer cells (by ejection of miRNA via EVs). We used miRTarBase to identify experimentally validated targets for each miRNA in our HPV⁺/⁻ enriched lists and used these transcripts in conjunction with DAVID to determine which signalling pathways would most likely be affected by the uptake or release of EV miRNA cargo. A number of overlapping pathways were shown to be targeted by miRNA enriched in EVs from HPV⁺ and HPV⁻ cells including PI3K-Akt, FoxO, HIF-1, mTOR and p53 signalling pathways (Table 2).

In the current study, we show for the first time the miRNA signature associated with EVs released by HPV⁺ and HPV⁻ OPSCC cells cultured *in vitro*. A number of miRNA were identified that were either enriched in HPV⁻ or HPV16⁺ cell derived EVs. We also identified miRNA that were highly abundant in all EVs, independent of HPV status of the producing cell. We found miRNA that were abundant in EVs from HPV+ OPSCC cells that had previously been reported as cargo of EVs from HPV18⁺ HeLa cervical carcinoma cells, including miR-99a-5p, miR-27a-3p and miR-27b-3p.¹³ Our data indicate that miR-99a-5p is enriched in EVs derived from HPV⁺ OPSCC. Whereas, miR-27a-3p and miR-27b-3p are abundant in EVs produced by HPV⁺ and HPV⁻ cells. The most highly enriched miRNA in HPV⁺ EVs was miR-363-3p, which has been shown to be the most differentially expressed miRNA when comparing HPV⁺ and HPV⁻ tonsillar squamous cell carcinoma ex vivo tissue sections.¹⁸ Two other members of the miR-106-363 cluster were enriched in HPV⁺ OPSCC-derived EVs, miR-106a-5p and miR-20b-5p/miR-20b-3p. miR-106a-5p and miR-20b-5p have recently been shown to be upregulated in breast cancer tissues and enriched in circulating serum EVs of breast cancer patients.¹⁹ miR-20b-5p has been described as a core HPV upregulated miRNA because it is consistently upregulated in HPV⁺ OPSCC²⁰ and cervical cancer tissues.¹⁸ Increased miR-20b-5p expression in cervical cancer is dependent on the viral E6 oncoprotein and has been shown to promote cancer cell invasion.²¹ However, expression of the normally silent miR-20b-5p and other miRNA cluster members (miR-106a-5p and miR-363-3p) caused a decrease in proliferation in oral squamous cell carcinoma cells ²², highlighting the cancer-specific role of certain miRNAs. We found an enrichment of miR-9-5p and miR-9-3p in HPV⁺ EVs, which is consistent with reports of their overexpression in HPV⁺ OPSCC²⁰ and HPV⁺ cervical cancer.²³

The most highly enriched miRNA in HPV⁻ EVs was miR-767-5p, which has been shown to be overexpressed in some tumours and to target members of the TET family of tumour suppressors.²⁴ miR-105-5p was similarly enriched in HPV⁻ EVs and has been reported to promote breast cancer metastasis by EV mediated targeting of endothelial cells.²⁵ We found that miR-100-5p was enriched in EVs derived from HPV⁻ OPSCC cells. Interestingly, Honegger et al. reported that cellular expression and packaging of miR-100-5p into EVs was increased in HeLa cells upon silencing of cellular E6/E7 viral oncogene expression.¹³ Cellular expression of miR-100-5p has previously been shown to be downregulated in response to HPV16/18 viral infection in an E6/E7 dependent manner.¹¹

The miRNA cargo of EVs represents a source of circulating biomarkers that may be useful in diagnosing and monitoring cancer. Our data shows that EVs contain overlapping miRNA profiles, but that certain miRNAs may be cancer and subtype specific. Indeed, unbiased hierarchical clustering of EV miRNA cargo grouped samples in this study based on the HPV-status of the producing cell. The detection of these EV-encapsulated miRNA signatures in biological fluids might be a suitable method for surveillance of OPSCC patients to detect catastrophic metastatic recurrence.

Acknowledgments

We would like to thank Angie Fawkes and the other members of the Edinburgh Clinical Research Facility for their support and technical expertise with small RNA sequencing experiments. None declared

Ethical approval

No human participants or animals were involved in this study

References

- Chaturvedi AK, Engels EA, Pfeiffer RM, et al. Human papillomavirus and rising
 oropharyngeal cancer incidence in the United States. *J Clin Oncol.* 2011;29(32):4294-4301.
- 2. Nasman A, Attner P, Hammarstedt L, et al. Incidence of human papillomavirus (HPV) positive tonsillar carcinoma in Stockholm, Sweden: an epidemic of viral-induced carcinoma? *Int J Cancer.* 2009;125(2):362-366.
- Lindel K, Beer KT, Laissue J, Greiner RH, Aebersold DM. Human papillomavirus positive squamous cell carcinoma of the oropharynx: a radiosensitive subgroup of head and neck carcinoma. *Cancer.* 2001;92(4):805-813.
 - Huang SH, Perez-Ordonez B, Weinreb I, et al. Natural course of distant metastases following radiotherapy or chemoradiotherapy in HPV-related oropharyngeal cancer. *Oral Oncol.* 2013;49(1):79-85.
 - Valadi H, Ekstrom K, Bossios A, Sjostrand M, Lee JJ, Lotvall JO. Exosome-mediated transfer of mRNAs and microRNAs is a novel mechanism of genetic exchange between cells. *Nat Cell Biol.* 2007;9(6):654-659.

6.

- D'Souza-Schorey C, Clancy JW. Tumor-derived microvesicles: shedding light on novel microenvironment modulators and prospective cancer biomarkers. *Genes Dev.* 2012;26(12):1287-1299.
- Ogawa Y, Taketomi Y, Murakami M, Tsujimoto M, Yanoshita R. Small RNA transcriptomes of two types of exosomes in human whole saliva determined by next generation sequencing. *Biol Pharm Bull.* 2013;36(1):66-75.
- Koppers-Lalic D, Hackenberg M, de Menezes R, et al. Noninvasive prostate cancer detection by measuring miRNA variants (isomiRs) in urine extracellular vesicles. *Oncotarget.* 2016;7(16):22566-22578.
- Ben W, Yang Y, Yuan J, et al. Human papillomavirus 16 E6 modulates the expression of host microRNAs in cervical cancer. *Taiwan J Obstet Gynecol.* 2015;54(4):364-370.
- Chiantore MV, Mangino G, Iuliano M, et al. Human papillomavirus E6 and E7 oncoproteins affect the expression of cancer-related microRNAs: additional evidence in HPV-induced tumorigenesis. *J Cancer Res Clin Oncol.* 2016;142(8):1751-1763.
- 11. Wang X, Wang HK, Li Y, et al. microRNAs are biomarkers of oncogenic human papillomavirus infections. *Proc Natl Acad Sci U S A.* 2014;111(11):4262-4267.
- 12. Honegger A, Leitz J, Bulkescher J, Hoppe-Seyler K, Hoppe-Seyler F. Silencing of human papillomavirus (HPV) E6/E7 oncogene expression affects both the contents and the amounts of extracellular microvesicles released from HPV-positive cancer cells. *Int J Cancer.* 2013;133(7):1631-1642.
 - Honegger A, Schilling D, Bastian S, et al. Dependence of intracellular and exosomal microRNAs on viral E6/E7 oncogene expression in HPV-positive tumor cells. *PLoS Pathog.* 2015;11(3):e1004712.

- 21. 22.
- Love MI, Huber W, Anders S. Moderated estimation of fold change and dispersion for RNA-seq data with DESeq2. *Genome Biol.* 2014;15(12):550.
 - Chou CH, Shrestha S, Yang CD, et al. miRTarBase update 2018: a resource for experimentally validated microRNA-target interactions. *Nucleic Acids Res.* 2018;46(D1):D296-D302.
 - 16. Huang da W, Sherman BT, Lempicki RA. Systematic and integrative analysis of large gene lists using DAVID bioinformatics resources. *Nat Protoc.* 2009;4(1):44-57.
 - Huang da W, Sherman BT, Lempicki RA. Bioinformatics enrichment tools: paths toward the comprehensive functional analysis of large gene lists. *Nucleic Acids Res.*2009;37(1):1-13.
 - Lajer CB, Garnaes E, Friis-Hansen L, et al. The role of miRNAs in human papilloma virus (HPV)-associated cancers: bridging between HPV-related head and neck cancer and cervical cancer. *Br J Cancer.* 2012;106(9):1526-1534.
 - 19. Li M, Zhou Y, Xia T, et al. Circulating microRNAs from the miR-106a-363 cluster on chromosome X as novel diagnostic biomarkers for breast cancer. *Breast Cancer Res Treat.* 2018;170(2):257-270.
 - 20. Hui AB, Lin A, Xu W, et al. Potentially prognostic miRNAs in HPV-associated oropharyngeal carcinoma. *Clin Cancer Res.* 2013;19(8):2154-2162.
 - Cheng Y, Geng L, Zhao L, Zuo P, Wang J. Human papillomavirus E6-regulated microRNA 20b promotes invasion in cervical cancer by targeting tissue inhibitor of
 metalloproteinase 2. *Mol Med Rep.* 2017;16(4):5464-5470.
 - 2. Khuu C, Jevnaker AM, Bryne M, Osmundsen H. An investigation into anti-proliferative effects of microRNAs encoded by the miR-106a-363 cluster on human carcinoma cells

and keratinocytes using microarray profiling of miRNA transcriptomes. *Front Genet.* 2014;5:246.

- 23. Park S, Eom K, Kim J, et al. MiR-9, miR-21, and miR-155 as potential biomarkers for HPV positive and negative cervical cancer. *BMC Cancer.* 2017;17(1):658.
- 24. Loriot A, Van Tongelen A, Blanco J, et al. A novel cancer-germline transcript carrying pro-metastatic miR-105 and TET-targeting miR-767 induced by DNA hypomethylation in tumors. *Epigenetics.* 2014;9(8):1163-1171.
- Zhou W, Fong MY, Min Y, et al. Cancer-secreted miR-105 destroys vascular endothelial barriers to promote metastasis. *Cancer Cell.* 2014;25(4):501-515.

Figure legends

Figure 1. Analysis of conditioned medium. Cells were allowed to condition EV-depleted medium for 24 h, which was then clarified by differential centrifugation. TRPS analysis was used to determine particle modal diameter (A), concentration (B) and size profile (C). Data represents the average of three independent experiments with error bars indicating SEM. Two-tailed unpaired t-test was performed (*p<0.05, **p<0.01, ****p<0.0001).

Figure 2. Characterisation of isolated EVs. Small EVs were purified by differential centrifugation and SEC. Modal diameters were measured by TRPS (A). EV lysates were examined by western blot using antibodies specific for GM130, CD63, TSG101 and CD9 (B). Size profiles were determined by TRPS (C). Numerical data is the average of 5 independent experiments with error bars indicating SEM. Western blot images are representative of three independent experiments. Figure 3. Characterisation of EV RNA cargo. RNA was extracted from EVs and size profile examined by Bioanalyzer (A-D). Small RNA sequencing identified a variety of RNA species (E), including miRNA of different abundance (F). EV miRNA cargo was correlated with HPV status of the producing cell (G).

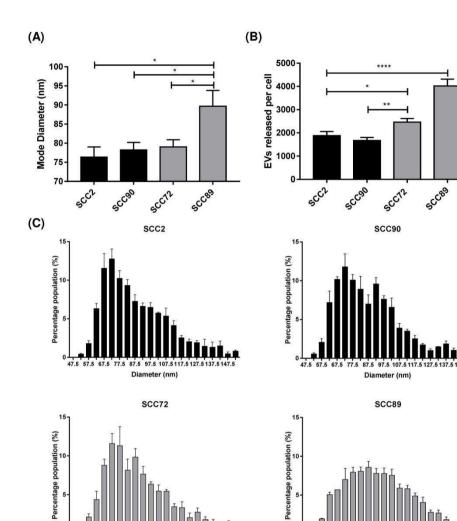
Figure 4. Validation of small RNA sequencing. miR-29b-3p and miR-20b-5p were identified as miRNA enriched in EVs derived from HPV- or HPV+ cells from small RNA sequencing data (A,D). RNA was extracted from EVs and subject to quantitative real-time PCR (QPCR) (B,E). The cellular miRNA expression level was measured by QPCR (C,F). For each repeat EVs were isolated from conditioned medium taken from three confluent T-175 flasks, per cell line. QPCR data was normalised to hsa-let-7a-5p and expressed relative to the sample with lowest target abundance. Data represents the average of two independent experiments with error bars indicating SEM.

Table 1. Differential abundance of miRNA in EVs from HPV⁺ and HPV⁻ cells. miRNA were identified that were enriched in EVs from HPV⁺ or HPV⁻ cells, or that were highly abundant in all EVs.

Table 2. Pathways predicted to be targeted by EV miRNA cargo. Experimental validated miRNA targets were used to predict which signalling pathways would be targeted by miRNA enriched in EVs from HPV⁺ and HPV⁻ cells.

miRNAs associated with HPV+			miRNAs associated w	miRNAs with >5000rpm in all samples						
miRNA hsa-miR-363-3p	log 2 FC	P value	miRNA hsa-miR-767-5p	log 2 FC -5.3	P value		RPM (Reads per million)			
	7.5	6.32E-14			1.18E-06	miRNA	SCC2	SCC90	SCC72	SCC89
hsa-miR-551b-3p	6.3	2.46E-10	hsa-miR-105-5p (hsa-mir-105-1)	-5.2	2.64E-06	hsa-miR-26a-5p	7921	15357	5356	6860
nsa-miR-20b-5p	5.6	1.95E-09	hsa-miR-105-5p (hsa-mir-105-2)	-5.1	5.35E-06	hsa-miR-27a-3p	24255	9168	60411	15430
nsa-miR-20b-3p	5.3	2.14E-06	hsa-miR-100-5p	-4.7	3.14E-06	hsa-miR-221-3p	8897	5656	9361	24874
hsa-miR-143-3p	4.0	1.30E-04	hsa-miR-584-5p	-4.4	1.10E-04	hsa-miR-20a-5p	6975	7112	15767	7136
hsa-miR-106a-5p	3.6	5.59E-05	hsa-miR-3065-5p	-2.9	1.64E-03	hsa-miR-23a-3p	88895	35957	133610	48130
hsa-miR-9-5p (hsa-mir-9-3)	2.9	3.87E-03	hsa-miR-338-3p	-2.9	1.64E-03	hsa-miR-26a-5p (hsa-mir-26a-1)	8502	17360	5831	7670
hsa-miR-9-5p (hsa-mir-9-2)	2.8	3.33E-03	hsa-miR-135b-5p	-2.7	8.73E-03	hsa-miR-30d-5p	10891	22220	20541	17182
hsa-miR-9-5p (hsa-mir-9-1)	2.8	2.99E-03	hsa-miR-589-5p	-2.6	1.79E-02	hsa-miR-3074-5p	9595	14679	12639	11646
hsa-miR-99a-3p	2.4	3.58E-02	hsa-miR-3065-3p	-2.5	9.03E-03	hsa-miR-27b-3p	11175	20100	13015	7334
hsa-miR-99a-5p	2.3	3.67E-02	hsa-miR-338-5p	-2.5	9.03E-03	At-				
hsa-miR-9-3p (hsa-mir-9-1)	2.3	2.50E-02	hsa-miR-1307-5p	-2.3	8.32E-03					
hsa-miR-193a-5p	2.2	1.83E-02	hsa-miR-29b-3p (hsa-mir-29b-1)	-2.2	1.78E-02					
hsa-let-7b-3p	2.0	4.58E-02	hsa-miR-29a-5p	-2.1	2.33E-02					
			hsa-miR-7-5p (hsa-mir-7-1)	-1.9	3.98E-02					
			hsa-miR-345-5p	-1.8	3.55E-02					
			hsa-miR-18a-5p	-1.8	2.54E-02					
			hsa-miR-615-3p	-1.8	4.57E-02					
			hsa-miR-1307-3p	-1.7	3.72E-02					

Pathways associated with HPV-EV miRNA					Pathways associated with HPV+ EV miRNA					
Pathway	N* of Genes % P-Value Benjamini-Hochberg Pathway		Pathway	N ^e of Genes	%	P-Value	Benjamini-Hochbe			
Pathways in cancer	14	27.5	2.50E-08	3.106-06	Pathways in cancer	30	35.1	4.90€-22	8.10€-20	
PI3K-Akt signaling pathway	13	25.5	5.80E-08	3.60E-06	FoxO signaling pathway	17	20.5	3.40E-15	1.10E-13	
MicroRNAs in cancer	12	23.5	8.40E-08	3.408-06	HF-1 signaling pathway	15	18.1	1.80E-14	5.10E-13	
FoxO signaling pathway	9	17.6	2.50E-07	6.00E-05	TNF signaling pathway	15	18.1	5.70E-14	1.30E-12	
Proteoglycans in cancer	9	17.6	5.10E-06	7.801-05	Proteoglycans in cancer	18	21.7	1.30E-13	2.70E-12	
Focal adhesion	9	17.6	6.40E-06	8.70E-05	PI3K-Akt signaling pathway	21	25.3	8.20E-13	1.40E-11	
Central carbon metabolism in cancer	5	9.8	2.80E-04	2.60E-03	Focal adhesion	16	19.3	4.30E-11	4.00E-10	
GMP-PKG signaling pathway	6	11.8	1.40E-03	9.20E-03	MicroRNAs in cancer	17	20.5	4.30E-10	3.60E-09	
HIF-1 signaling pathway	5	9.8	1.40E-03	9.10E-03	Apoptosis	10	12	1.108-09	7.80E-09	
Transcriptional misregulation in cancer	6	11.8	1.40E-03	8.70E-03	T cell receptor signaling pathway	11	13.3	7.00E-09	4.00E-08	
Choline metabolism in cancer	5	9.8	1.60E-03	9.20E-03	Toll-like receptor signaling gathway	11	13.3	9.30E-09	5.10E-08	
Sphingolipid signaling pathway	5	9.8	3.00E-03	1.30E-02	mTOR signaling pathway	9	10.8	1.608-08	8.10E-08	
mTOR signaling pathway	4	7.8	3.00E-03	1.30E-02	Sphingolipid signaling pathway	11	13.3	3.10E-08	1.50E-07	
AMPK signaling pathway	5	9.8	3.20E-03	1.308-02	Central carbon metabolism in cancer	9	10.8	3.50E-08	1.60E-07	
Apoptosis	4	7.8	3.70E-03	1.506-02	AMPK signaling pathway	11	13.3	3.608-08	1.70E-07	
p53 signaling pathway	4	7.8	4.60E-03	1.70E-02	ErbB signaling pathway	9	10.8	4.00E-07	1.50E-06	
Hippo signaling pathway	5	9.8	6.80E-03	2.50E-02	B cell receptor signaling pathway	8	9.6	1.108-05	4.00E-06	
TGF-beta signaling pathway	4	7.8	8.60E-03	3.00E-02	Choline metabolism in cancer	9	10.8	1.308-05	4.20E-06	
	1			l secondo l	Jak-STAT signaling pathway	10	12	2.00E-06	6.70E-06	
					Viral carcinogenesis	11	13.3	4.50E-05	1,50E-05	
					MAPK signaling pathway	12	14.5	4.70E-05	1.50E-05	
					MEGF signaling pathway	7	8.4	8.50E-06	2,60E-05	
					cAMP signaling pathway	10	12	2.60E-05	7.10E-05	
					Rap1 signaling pathway	10	12	4.10E-05	1.10E-04	
					Transcriptional misregulation in cancer	9	10.8	5.40E-05	1.40E-04	
					Ras signaling pathway	10	12	7.206-05	1.80E-04	
					p53 signaling pathway	6	7.2	1.90E-04	4.60E-04	
					NF-kappa B signaling pathway	6	7.2	5.50E-04	1.50E-03	
					NOD-like receptor signaling pathway	5	5	9.70E-04	2.20E-03	
					Leukocyte transendothelial migration	5	7.2	2.508-03	5.30E-0.3	



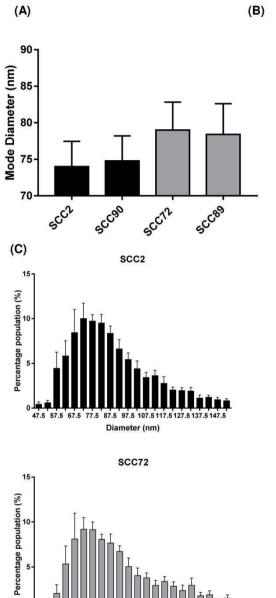
47.5 57.5 67.5 77.5

87.5 97.5 107.5 117.5 127.5 137. Diameter (nm)

47.5 57.5 67.5 77.5

87.5 97.5 107.5 117.5 127.5 137 Diameter (nm)





87.5 97.5 107.5 117.5 127.5 137.5

Diameter (nm)

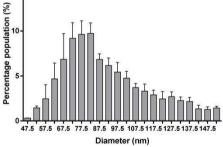
SCC2 EV CL GM130 CD63 TSG101 CD9 SCC90 15-Percentage population (%) 0 47.5 57.5 67 5 87.5 97.5 107.5 117.5 127.5 137.5 147. Diameter (nm) SCC89 15

SCC90

EV CL SCC89 EV CL

SCC72

EV CL



0 47.5 57.5 67.5 77.5

